
This is an electronic reprint of the original article.
This reprint may differ from the original in pagination and typographic detail.

Author(s): Miksic, A. & Alava, Mikko J.

Title: Evolution of grain contacts in a granular sample under creep and stress relaxation

Year: 2013

Version: Final published version

Please cite the original version:

Miksic, A. & Alava, Mikko J. 2013. Evolution of grain contacts in a granular sample under creep and stress relaxation. *Physical Review E*. Volume 88, Issue 3. 032207/1-7. ISSN 1539-3755 (printed). DOI: 10.1103/physreve.88.032207.

Rights: © 2013 American Physical Society (APS). This is the accepted version of the following article: Miksic, A. & Alava, Mikko J. 2013. Evolution of grain contacts in a granular sample under creep and stress relaxation. *Physical Review E*. Volume 88, Issue 3. 032207/1-7. ISSN 1539-3755 (printed). DOI: 10.1103/physreve.88.032207, which has been published in final form at <http://journals.aps.org/pre/abstract/10.1103/PhysRevE.88.032207>.

All material supplied via Aaltodoc is protected by copyright and other intellectual property rights, and duplication or sale of all or part of any of the repository collections is not permitted, except that material may be duplicated by you for your research use or educational purposes in electronic or print form. You must obtain permission for any other use. Electronic or print copies may not be offered, whether for sale or otherwise to anyone who is not an authorised user.

Evolution of grain contacts in a granular sample under creep and stress relaxationA. Miksic^{1,2,*} and M. J. Alava²¹*Istituto dei Sistemi Complessi – CNR, Area di Ricerca di Roma-Tor Vergata, Via del Fosso del Cavaliere 100, 00133 Roma, Italy*²*COMP Centre of Excellence, Department of Applied Physics, Aalto University, P.O. Box 11100, 00076 AALTO, Finland*

(Received 31 January 2012; revised manuscript received 19 July 2013; published 27 September 2013)

This article deals with the characterization, using an acoustic technique, of the mechanical behavior of a dry dense granular medium under quasistatic loading. Ultrasound propagation through the contact-force network supporting the external load offers a noninvasive probe of the viscoelastic properties of such heterogeneous media. First the response of a glass bead packing is studied in an oedometric configuration during creep and relaxation tests. Quasilogarithmic increases of sound velocities are found in both mechanical tests. A model based on the mechanics of microcontacts between rough grains adequately reproduces our experimental results, especially for the evolution of elastic modulus. Another main experimental finding is that collective grain rearrangements within the packing also play a crucial role at the early stage of creep and relaxation.

DOI: [10.1103/PhysRevE.88.032207](https://doi.org/10.1103/PhysRevE.88.032207)

PACS number(s): 45.70.Cc, 43.58.+z, 62.20.-x

I. INTRODUCTION

Granular assemblies are random arrangements of discrete grains for which sizes can vary and are larger than $1\ \mu\text{m}$. With such a wide definition, granular media are obviously ubiquitous in our daily lives, but, despite this apparent simplicity, present us with fundamental physics problems. In particular, granular media, as any other material, undergo aging with time, like creep under a constant applied load or stress relaxation when the deformation state is fixed. Relaxation phenomena and even more creep have been extensively studied in heterogeneous geomaterials, such as rocks or sands [1–3] mostly in triaxial configuration [4,5]. However, the physical mechanisms, from which creep and relaxation in granular media derive, are still under debate.

In the case of dry cohesionless granular materials, the contacts between particles are nonlinear, repulsive, and frictional and a geometrical disorder exists in these granular packings [6]. A direct consequence of this is the strong local heterogeneity of the stress distribution within the medium [7]. Since Dantu [8] and De Josselin de Jong [9], we already know that the distribution of the contact forces, resulting from an externally applied load, is very inhomogeneous [10,11], as shown in experiments by photoelastic visualization [9,11,12] and via simulations [10,13]. The contact network determines most salient mechanical properties of a dense granular medium such as its ability to bear load, its nonlinear elastic response, and flow behavior.

This contact network, which seems to be the key for the mechanical response, is not easy to investigate within real three-dimensional granular media. In this context, using acoustic waves provides a unique noninvasive probe of both the structure and the nonlinear elastic properties of the force network [14,15] in a granular sample. At high frequency, the wavelength is about the size of the grains and the ultrasound wave is extremely sensitive to spatial fluctuations in the force network. The acoustic wave is scattered by the many heterogeneities of the granular medium, hence the name “multiple scattered” wave for this acoustic speckle pattern.

The signal associated to this wave type is specific to each granular configuration [14]. At low frequencies, such that the wavelengths are much larger than the grain size, the granular medium is seen as a homogeneous continuum by the propagating wave. This ballistic wave at low frequency does not change with the granular medium configuration and is reproducible for a given protocol of sample preparation [14]. Measuring the elastic wave velocity in this case gives access to the elastic modulus of the granular medium [16,17].

In the present article, we compare two types of experiments on dry cohesionless granular samples: (i) creep at a fixed load and (ii) stress relaxation under a constant deformation. A common question is: What happens at the meso- and microscopic levels of the particle contacts and the force network that could explain the macroscopic mechanical responses of the samples under these two different loadings? Are there universal characteristics? Which are the physical mechanisms involved? In both kinds of tests, the evolution of grain contacts is monitored via a method of wave propagation. Granular sample, experimental setup and methods are described in detail in a first part. The experimental results for creep and relaxation experiments are then outlined and discussed in the following section. Similar effects from creep and relaxation are observed on the stiffness of granular sample. Two major physical mechanisms are highlighted by comparing experimental data to different models. Conclusions finally close the article.

II. EXPERIMENTS

In order to follow the evolution of contacts inside the granular materials, we developed a setup coupling the mechanical test with the ultrasonic measurement. A schematic picture of the experiment is illustrated in Fig. 1. Spherical glass beads of a diameter between 300 and 400 μm are filled by rain deposition in a cylindrical cell up to 18 mm in height. The cell is closed at the top and bottom surfaces by two fitting transducers of diameter 30 mm. The top piston applies a controlled vertical load to the sample and the axial displacement, as a function of the applied load, induces a macroscopic uniaxial strain of the granular sample, since the container wall is presumed

*amandinemiksic@yahoo.fr

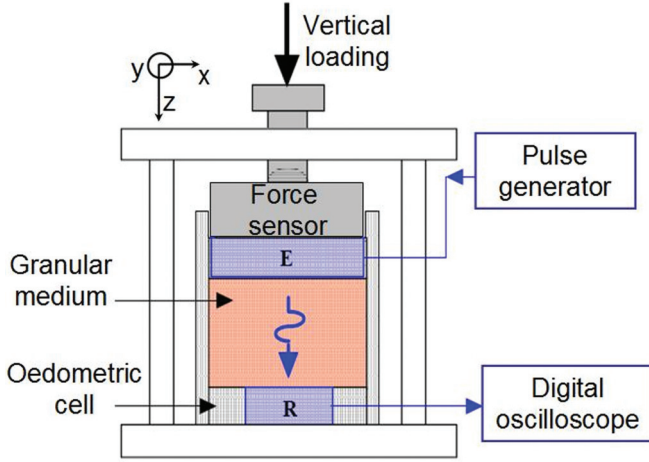


FIG. 1. (Color online) Device for the propagation of an acoustical wave during granular sample compression; E is used for emitting transducer and R is the receiver.

to be rigid enough to avoid lateral motion (oedometric configuration).

Before a test, a sample is subjected to a preloading up to $\sigma_{zz} = 650$ kPa, in order to obtain a better reproducibility and an initial jammed state of the granular medium. After this preloading step, the sample density is $0.655 \pm 0.9\%$, slightly higher than random close packing, due to dispersity. Then a load from 10 kPa to $\sigma_{zz}^{\max} < 630$ kPa is applied at a constant strain rate. When σ_{zz}^{\max} is reached, either the strain is fixed during a waiting time t_w , in order to observe the stress relaxation in the sample, or the stress is kept constant leading to a creep test where deformation increases with time. After the chosen duration t_w , between 2 s and 2 h, the sample is completely unloaded.

Sets of experiments were performed in which everything is similar in all but the value of one parameter. As a first parameter, different values of strain rates were used during the loading stage: $2.8 \times 10^{-3}\%$ s $^{-1}$, $8.3 \times 10^{-3}\%$ s $^{-1}$, $2.8 \times 10^{-2}\%$ s $^{-1}$, and $8.3 \times 10^{-2}\%$ s $^{-1}$. Then the maximal stress, at the beginning of relaxation or during creep, is applied up to the values of 627, 470, or 313 kPa. We should note that our measurements are realized at much lower stress than the value required to produce the grain fracture of about 20 MPa for the glass beads [18] and indeed no particle breakages are observed. Lastly the influence of wear surface state of glass beads was also investigated: The “new beads” have not suffered any treatment, in opposition to the “worn beads” which had already gone through 200 loading cycles or “very worn beads” that endured 2000 cycles. We used spherical beads made of chemically inert glass; therefore we exclude chemical bonds between particles [19] or grains angularity [20] as the origin of the aging. We study the relative variation $\Delta x = [x(t) - x_0]/x_0$ of variable x after the time t , compared to the initial value x_0 at the beginning of the creep or relaxation stage; x is either creep strain ε_{zz} or relaxed stress σ_{zz} . Reproducibility was measured on sets of at least 12 similar tests; data dispersion is displayed as error bars.

The acoustic experiment consists in sending a brief pulse by mean of an ultrasonic transducer. This compression pulse excites a broadband of frequencies centered at 500 kHz. The

acoustical signal, transmitted through the granular sample, is received by an identical piezoelectric transducer and recorded. The usual signal presents two components: a sinusoidal component (first peak and valley) from the ballistic propagation of the pulse; then some oscillations appear as echoes. The received signal is around 90–120 kHz.

The oedometric elastic modulus related to the velocity V of the longitudinal wave propagating along the vertical (z axis) direction is obtained via

$$E_{\text{oed}} = \rho_{\text{app}} V^2, \quad (1)$$

where $\rho_{\text{app}} = m/(Sh)$ is the apparent volumetric mass of a granular sample of mass m , height h , and surface area S . The instantaneous wave velocity is calculated from the sample's height and the time of flight T_f as

$$V = h/T_f. \quad (2)$$

Since the total mass of glass beads ($m \sim 23$ g) inside the container and the surface area S are constant, the change in elastic modulus is related only to the time of flight T_f and the height h :

$$dE_{\text{oed}}/E_{\text{oed}} \approx dh/h + 2dT_f/T_f. \quad (3)$$

As we studied relative change with waiting duration, the absolute value of the time of flight T_f is not necessary and an intersection of the signal with zero reference is used for a better accuracy, as shown in Fig. 2.

We should note here that the elastic modulus deduced from the velocity of the propagated wave is usually found higher than the value defined from the local slope of the mechanical stress-strain curve. Indeed, this latter value could be around five to ten times smaller than the modulus obtained with the acoustical method. Such discrepancies between so-called static and dynamic moduli, in various granular materials, soils and rocks, have been already widely reviewed in the literature for a long time and the value of the elastic modulus obtained from the velocity of propagation of an acoustic pulse or wave is found to always be higher than the value from mechanical measurements [21–25]. As a matter of fact, the dynamic and static moduli can be equal only in the limit of the elastic domain, which corresponds to deformation lower than 10^{-5} in

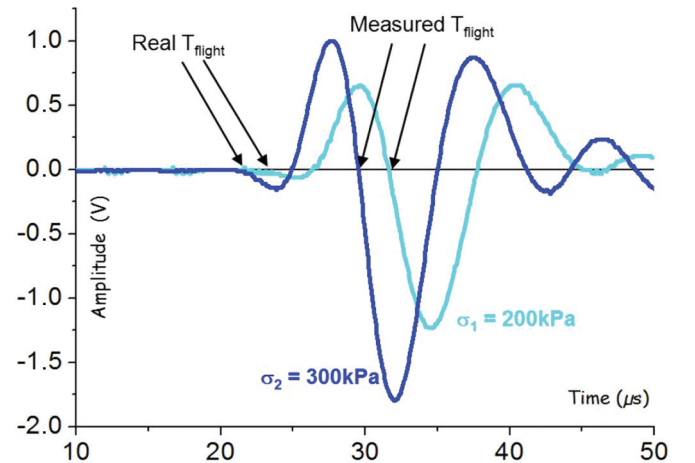


FIG. 2. (Color online) Received acoustical signal for two different stresses and determination of the time of flight.

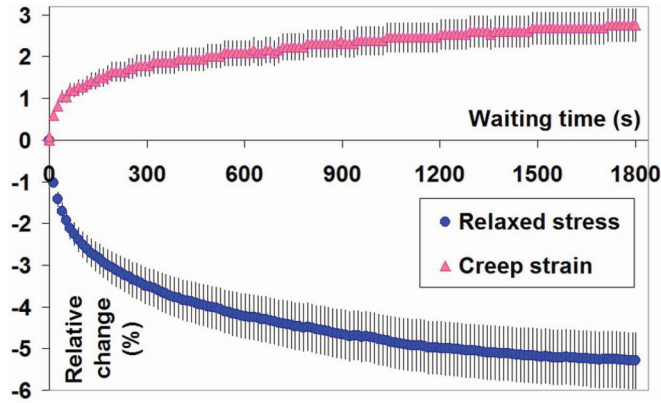


FIG. 3. (Color online) Relative change (negative) in stress for relaxation tests and relative change (positive) in compressive strain during creep vs waiting time (30 min). Tests are compared for two samples of new glass beads with an initial or constant applied stress of 627 kPa after a load at strain rate of $2.8 \times 10^{-3} \%$ /s.

the case of granular samples under uniaxial loading [26–29]. Such small deformation could not be reached with the setup used for the experiments presented in this article, and the samples undergo larger deformation. The local slope of the stress-strain curve for this case is no longer a correct definition for the elastic modulus, and the acoustic method gives a unique possibility of accessing the elastic constant.

III. RESULTS AND DISCUSSION

A. Similarity in creep and relaxation: Increase of stiffness with time

Figure 3 presents the typical relative changes in deformation for creep tests or in stress for relaxation tests and, in parallel, the relative change in the wave’s speed is observed for both tests in Fig. 4.

First of all, the most important result is that wave velocity increases in both tests: A stiffening of the granular sample occurs in parallel to the increasing creep strain but also during stress relaxation. During creep, one can argue that

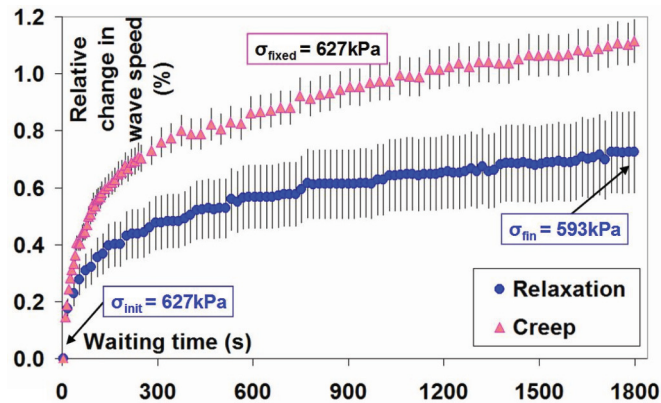


FIG. 4. (Color online) Relative change in wave speed for relaxation and creep tests vs waiting time (30 min). Tests are compared for two samples of new glass beads with an initial or constant applied stress of 627 kPa after a load at strain rate of $2.8 \times 10^{-3} \%$ /s.

the propagating distance of sound is shortened when strain develops under compression. But the diminution of sample height cannot explain the increase in wave velocity as the relative change of height is around ten times smaller than the change in wave speed [cf. Eq. (3)]. More surprisingly, the wave propagates faster even though the stress decreases during relaxation experiments. According to the effective medium theory [16,17], for ballistic sound propagation in the nonlinear elasticity case, the wave velocity increases as a power law of the applied stress:

$$V \approx (z\Phi)^{1/3} \sigma^{1/p}. \tag{4}$$

z is the coordination number (average number of contacts per grain) and Φ is the solid volume fraction in granular samples. Even if relaxation is not a case of nonlinear elasticity, it remains surprising at a first sight that wave celerity and stress can evolve in opposite ways.

During creep, samples generally compress by several micrometers—around $7 \mu\text{m}$ maximum; the compressive strain $\epsilon_{zz}(t)$ is around 1% at 627 kPa after loading, and after 4 h of creep ϵ_{zz} displays a maximum value of 1.05%. The relative change in creep strain $\Delta\epsilon_{zz}$ is 9% for a sample of new beads after 4 h of creep, and the corresponding wave speed presents a relative increase of 2.8%, from an initial absolute value of around 810 m/s. In relaxation tests, stress decreases at around 13% after 2 h and the relative increase of ultrasound wave celerity is 1.2%.

Moreover, the response of the granular sample depends on a few parameters. First, the strain rate applied during the loading stage has a huge influence on the relative change in relaxed stress σ or creep strain ϵ and on the wave velocity in parallel. In all cases, a higher loading rate induces larger variations. A similar effect of the loading speed before creep was observed in [30]. A slow application of load allows the granular material to reach at every moment a state of relative equilibrium, while a fast loading does not allow enough time for the viscous (deferred) strain to occur. After a slow loading, the medium has less opportunity to deform; the evolution of ϵ or σ , and of the wave speed are therefore smaller. The viscosity of the glass beads packing which is involved comes probably from the contacts between grains, where stresses are high because of small contact surface areas.

Secondly, the wear surface state of glass beads is important: All the relative changes are smaller for samples of worn beads than of new ones. New glass beads present surface asperities, while the worn beads are less rough and smoother, as their asperities have been flattened during compression cycles. The samples with worn beads display smaller creep deformation or stress relaxation than those with new beads. In the same vein, experiments from [30] show that the angularity and microroughness of sand lead to a response which is less stable and more time dependent than with spherical glass beads.

Lastly, we observed that the initial or imposed stress has a large effect, as reported in the literature [5,20,30,31]. The stress change in relaxation tests is all the more important when the initial imposed stress is high. Likely, creep strain is greater for a higher confining pressure. On the contrary, a lower stress value leads to a larger relative change of the wave celerity, i.e., in elastic modulus. This can be understood in the following

way: At a low stress, the network of contacts is less dense and a small change in the contact area will have a strong effect. At a high stress, the wave propagation is faster because the material is more rigid and all the beads' contacts are already overstressed. Therefore, a small change will be less significant when the granular sample is heavily loaded.

In this part, similar trends have been observed in creep and relaxation. As similar mechanical behaviors are produced in both cases, identical mechanisms should be at the origin of creep and relaxation phenomena in the granular material.

B. Solid friction for a multiple contact interface

In creep and relaxation, the microcontacts between grains are important. Bréchet and Estrin suggested a model for time-dependent friction of ductile materials [32], used later in many studies on solid friction [33–35]. The model is built for a multiple contact interface via asperities of rough solids, and the evolution of the multiple contacts between grains in a granular sample can be understood then by analogy. The evolution of friction coefficients is proportional to the logarithm of the time during which solids are kept in contact and a similar relationship is used for asperities heights:

$$h(t) = h_0\{1 - A \ln[1 + (t/\tau)]\}. \quad (5)$$

$h(t)$ is the height of asperities after a waiting time t under an applied uniaxial stress σ , and h_0 is the initial height. The parameter A , corresponding to the effective strain rate sensitivity, and the characteristic time τ are both dependent on material and temperature. Because of constancy of volume in plastic deformation, the contact area a^2 is linked to the asperities' height ($a^2 \sim h$) and therefore follows the same evolution with time as in [32]. As the global stiffness M of a granular sample is directly proportional to the surface areas of contacts [36], the logarithmic relationship was checked against the relative change of oedometric elastic modulus:

$$\frac{M(t) - M_0}{M_0} = \alpha \ln[1 + (t/\tau)]. \quad (6)$$

Figure 5 shows the suggested fit applied to the relative variation of modulus for the same two experiments of Fig. 4. The equation of the fits and correlation coefficients R^2 of

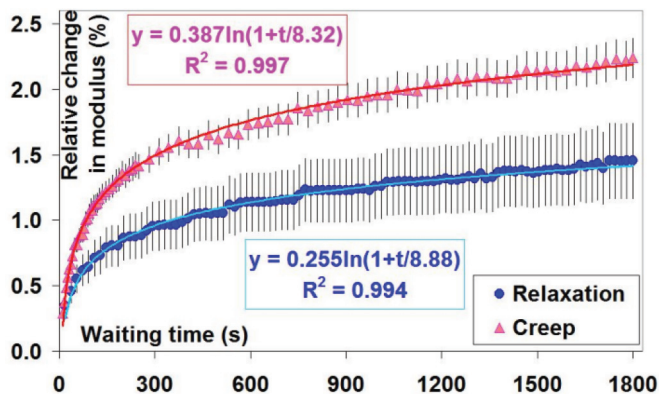


FIG. 5. (Color online) Relative change in oedometric modulus vs waiting time (30 min). Tests details: cf. Fig. 3. Logarithmic fits with equations and correlation coefficients are shown.

TABLE I. Fitting parameters and correlation coefficient for curves of relative change in modulus with time for 1 h tests on worn out (2000 cycles) glass beads with different applied stress after a load at strain rate $8.3 \times 10^{-3}\%/s$: for creep tests and relaxation tests respectively.

Creep tests					
Applied stress (kPa)	α	Error α	τ	Error τ	R^2
627	0.270	8.8×10^{-4}	0.69	0.02	0.996
470	0.368	1.3×10^{-3}	2.27	0.05	0.996
313	0.510	2.0×10^{-3}	10.68	0.22	0.996
Relaxation tests					
Initial stress (kPa)	α	Error α	τ	Error τ	R^2
627	0.114	8.6×10^{-4}	0.56	0.03	0.975
470	0.194	1.6×10^{-3}	2.72	0.13	0.958
313	0.340	1.8×10^{-3}	5.84	0.15	0.984

the approximation with experimental curves are specified. In the case of creep, as well as for the relaxation test, Eq. (6) fits the experimental data very well. Initial values for the oedometric modulus are between 130 and 210 MPa at the beginning of the waiting stage for the different tests. The values of the fitting parameters are close for both kinds of experiments when performed under same conditions, but the fit for creep curves is always better than in the relaxation case. The characteristic time τ depends strongly on the waiting duration, the strain rate during load, the stress level, and the utilized beads, as shown in Table I; τ varies widely from 0.5 to 20 s. On the contrary, the effective strain rate sensibility α is always between 0.1 and 0.6. This logarithmic approximation with only two adjustable parameters fits most of the data curves very well.

On the other hand, the fact that the evolution of creep deformation in granular media has a logarithmic shape is widely recognized in the literature [4,37], which offers mostly phenomenological studies on creep. The logarithmic fit (5) was checked first against the decrease of the sample's height during creep (Fig. 6) and relative change of creep strain (proportional to the relative change of height) was then checked. As a clear resemblance between creep and relaxation phenomena has been previously highlighted, the relative change in relaxed

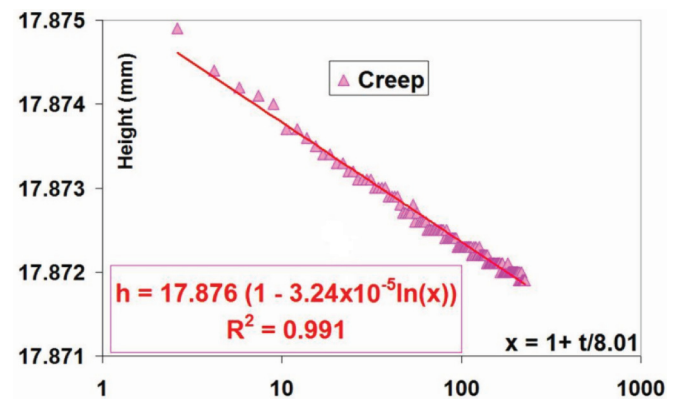


FIG. 6. (Color online) Height vs time normalized by characteristic time. Creep test from Fig. 4. Logarithmic fit with equation and correlation coefficient is displayed.

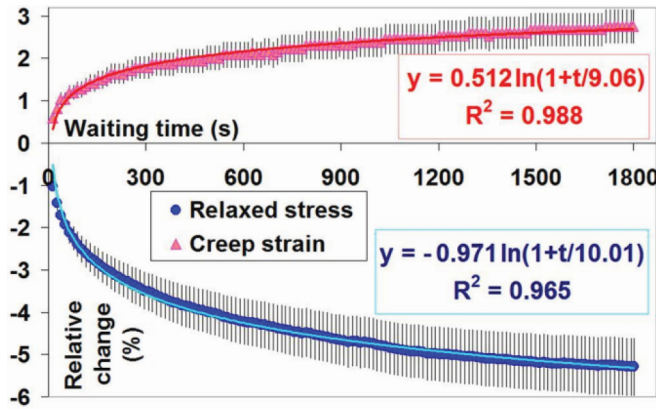


FIG. 7. (Color online) Relative change (negative) in stress for relaxation tests and relative change (positive) in compressive strain during creep vs waiting time (30 min). Tests details: cf. Fig. 4. Logarithmic fits with equations and correlation coefficients are displayed.

stress has been compared to fit (6) as well. Figure 7 displays fits on data from Fig. 4.

The characteristic times τ for the relative variation of relaxed stress or creep strain varies less than that for elastic modulus. Indeed, τ is only between 2 and 20 s for mechanical data (relative change in σ or ϵ) in both kinds of tests. Moreover the range width of these quantities is larger for relaxation than for creep experiments. However, the logarithmic approximation agrees much better with the data for the elastic modulus, than the relative change in relaxed stress or creep strain.

The good agreement of the modulus data with the fit from this model proves that considering friction between rough solids, at the microscopic level of grain contacts, is meaningful and could explain the evolution of stiffness in the granular sample, but not enough to understand the entire mechanics of the granular sample.

C. Response in two steps with different physical origins

The previous logarithmic fit is not, however, well adapted to the mechanical data curves for short experiments (few minutes) or at the start of long tests of creep and relaxation: A clear deviation appears, as shown in Fig. 8. The correlation coefficient between the fit with Eq. (6) and the data curve becomes much lower than 0.8. Therefore this logarithmic model is not enough anymore; it implies that another mechanism is probably involved at short times and the evolution with time includes different phases. Indeed, such mechanical response with different steps appears generally in creep of granular soils [4]. Primary creep, during which a first consolidation occurs, is defined for a decreasing strain rate. In secondary creep, strain increases as a logarithm of time and pure creep deformations occur in the granular skeleton. Deformations come from rearrangements over time due to sliding and rolling between particles. Tertiary creep is defined when strain rate increases and strain accelerates before failure.

For stress relaxation experiments, a mechanical behavior in two steps also exists [38]. Two distinct stages could appear in the granular material under relaxation where the

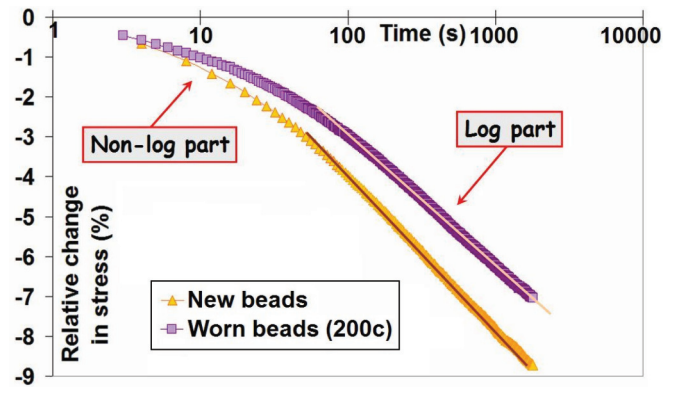


FIG. 8. (Color online) Relative change in stress vs waiting time (30 min). Relaxation tests are compared for two samples of new or worn (200 cycles) glass beads with an initial applied stress of 627 kPa after a load at strain rate of $8.3 \times 10^{-3} \%$ /s.

underlying physical mechanisms are different, as supported by simulations [38,39]. A slow stress relaxation fits well with logarithmic evolution in time and originates in the collective rearrangement of many grains via sliding and resultant “aging.” In the case of a fast application of load, a rapid evolution of stress exists before the slow logarithmic relaxation. The stress shows first a fast exponential relaxation in time (Fig. 9), attributed to a single particle relaxation mechanism. An approximation law with four parameters was proposed in [39] for stress variation in time:

$$\Delta\sigma(t)/\Delta\sigma(0) = A + B \exp(-t/\tau_1) - C \ln(t). \quad (7)$$

$\Delta\sigma(0)$ is the initial increment of stress when a small increment of strain is applied to the jammed granular sample and $\Delta\sigma(t)$ is the stress after a duration “ t ” of relaxation. τ_1 is a characteristic time, A and B are constants which depends on the material, and C sets the rate of the slow relaxation. In both relaxation and creep experiments, the deformation of the granular material is a combined result of rearrangements of particles in the granular sample and creep at grain contacts.

A simple $\log_{10}(t)$ variation is used in [38] and [4], but the response of the granular sample at long times is better approximated by a logarithm including a characteristic time

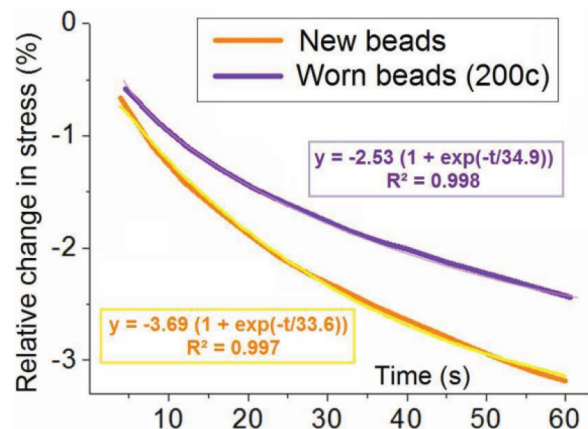


FIG. 9. (Color online) Relative change in stress vs waiting time for the first minute of previously presented tests; exponential fits with equations and correlation coefficients are displayed.

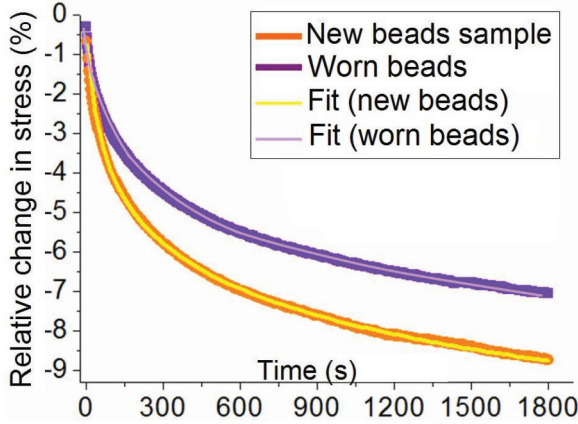


FIG. 10. (Color online) Relative change in stress for a relaxation test of 30 min on worn glass beads after a loading applied at strain rate of $8.3 \times 10^{-3} \%$ /s up to 627 kPa; approximation curve with four fitting parameters (see Table II) are visible.

[Eqs. (5) and (6)], as we have seen in the previous results. On the contrary, the exponential law fits our data much better than the logarithmic one, for the start of the curve or in the case of short experiments, as shown by the example of Fig. 9. As inspired from the model with Eq. (7) that takes into account both stages observed on the graphs (exponential for short time and logarithmic in long term), while keeping the idea that a characteristic time is associated with each step, the solution adopted here was

$$\%x(t) = A(1 - e^{-t/\tau_1}) \pm B \log_{10}(1 + t/\tau_2) \quad (8)$$

(where the variable x represents either σ or ε , in which case the second term is negative or positive, respectively). This approximation law includes four adjustable parameters, as in Eq. (7), and is the best outcome for all data of relative changes in stress or strain as a function of time. Indeed this model can fit perfectly the rapid change of data for short time (typically one or a few minutes), as well as the smooth variation in stress or strain for long-lasting experiments, with correlation coefficient always higher than 0.99. Considering all the different experiments we realized, the value of characteristic time τ_1 is spread between 15 and 265 s, whereas the range for τ_2 is only from 4 to 10 s. Figure 10 shows an example of this fit for a relaxation test of 30 min on samples of new or worn glass beads; the fitting parameters and the correlation coefficients are given in Table II.

The value of the characteristic time τ_1 in the exponential is always higher than the τ_2 of the logarithmic portion. The ratio τ_1/τ_2 can take values ranging from 3 to 11. However, the characteristic times may be associated with the ratio

TABLE II. Fitting parameters with errors and correlation coefficients R^2 for curves in Fig. 10.

Sample	Coeff.	A	τ_1	B	τ_2	R^2
New beads	Values	1.25	27.81	-1.68	6.47	0.999
	Errors	± 0.11	± 0.36	± 0.03	± 0.10	
Used-up beads	Values	1.17	14.08	-1.46	4.60	0.999
	Errors	± 0.02	± 0.62	± 0.09	± 0.32	

of viscosity to the shear elastic modulus. The relaxation mechanism of the particles is followed by the collective rearrangement of the grains due to sliding against each other. Viscosity of the glass beads at the contacts therefore plays a crucial role in the first part and then, during the logarithmic slow evolution, friction and sliding dominate, while the viscosity decreases relative to the spatial reorganization of the beads that gradually becomes more important. This second process is less viscous but more plastic.

D. CONCLUSIONS

In summary, we have studied the mechanisms at the origin of creep and relaxation in dry glass bead packings, using ultrasonic measurements to follow the evolution of contacts inside the granular material. Strong similarities in the experimental results in creep and relaxation have been highlighted. In both cases, the wave celerity increases with time, although the creep strain increases with time when the sample creeps under fixed load, whereas the stress decreases with time in the latter case, where the sample responds to a fixed strain rate. In particular, the relative change in wave speed is bigger when the waiting time is long, the glass beads are new, the loading is fast, and the initial or imposed stress is high. These results prove the existence of a certain viscoplasticity of the granular material and the importance of the phenomena at grain-grain contacts.

A model for solid friction at a multicontact interface [32] was tested on the experimental results, via the approximation curves for the elastic modulus and for the strain or stress variation. This approach of logarithmic type with a characteristic time fits our data on elastic modulus well, but applies with less relevance to the evolution of the relaxed stress and creep strain. Instead, the approximation with decreasing exponential seems more suitable to the mechanical data for short tests or just at the beginning of long ones.

To these two different experiments (creep and relaxation), we have applied a single model with two characteristic times and we have clearly highlighted two steps in the mechanical behavior of the compressed granular material. Indeed, the analysis of the experimental curves determines the coexistence of two mechanisms as suggested in [38]: a viscous mechanism which, at the scale of the granular packing, is linked to a viscous behavior at the grain contacts, and a mechanism of gradual rearrangement of grains, which results from plastic behavior of the assembly, which also depends on time. The study of the characteristic times associated with these two mechanisms, as well as the shape of the curves of evolution versus time, shows that the viscous mechanism is predominant at the beginning of a test and then yields to the second mechanism.

Moreover, mechanical and acoustic curves exhibit different behaviors, with characteristic times which appear different, suggesting that several aging mechanisms must coexist. A first characteristic time is associated with the rapid change at the beginning of the test, linked with friction of the glass beads at the contact areas. A second one is lower and corresponds to the evolution at long times, where the rearrangement of grains becomes important. An additional time constant can be hypothesized, corresponding either to the transition from

primary to secondary creep or to the transition from the first to the second physical mechanisms outlined above. A more thorough study would be needed to determine this definitively. Finally, one last time constant may characterize the hardening of the granular sample. This study demonstrates the complexity of granular media at different scales.

ACKNOWLEDGMENTS

The experiments were conducted under the supervision of Professor Xiaoping Jia at LPMDI laboratory in Paris-Est University, Champs-sur-Marne, France. We sincerely thank Dr. Juha Koivisto and Dr. Fergal Dalton for their kind support.

-
- [1] Q. Sun, H. F. Duan, L. Xue, and L. Qin, *Adv. Mater. Res.* **194-196**, 2031 (2011).
- [2] D. Amitrano and A. Helmstetter, *J. Geophys. Res. B* **111**, B11201 (2006).
- [3] L. Jian-Zhong, P. Fang-Le, and X. Lisheng, *Int. J. Geom.* **9**, 43 (2009).
- [4] M. Liingaard, A. Augustesen, and P. Lade, *Int. J. Geomech.* **4**, 157 (2004).
- [5] P. Lade, C. Liggio, and J. Nam, *J. Geotech. Geoenviron. Eng.* **135**, 941 (2009).
- [6] E. Guyon, *Phys. A (Amsterdam, Neth.)* **357**, 150 (2005).
- [7] D. M. Mueth, H. M. Jaeger, and S. R. Nagel, *Phys. Rev. E* **57**, 3164 (1998).
- [8] P. Dantu, in *Proceedings of the 4th International Conference on Soil Mechanics and Foundation Engineering* (Butterworths, London, 1957), Vol. 1, pp. 144–148.
- [9] A. Drescher and G. de Josselin de Jong, *J. Mech. Phys. Solids* **20**, 337 (1972).
- [10] B. Tighe and T. Vlugt, *J. Stat. Mech.* (2011) P04002.
- [11] J. Liu, Q. Sun, and F. Jin, *Front. Archit. Civ. Eng.* **4**, 109 (2010).
- [12] J. Wambaugh, R. Hartley, and R. Behringer, *Eur. Phys. J.* **32**, 135 (2010).
- [13] P. Wang, C. Song, C. Briscoe, K. Wang, and H. Makse, *Physica A* **389**, 3972 (2010).
- [14] X. Jia, C. Caroli, and B. Velicky, *Phys. Rev. Lett.* **82**, 1863 (1999).
- [15] E. T. Owens and K. E. Daniels, *Europhys. Lett.* **94**, 54005 (2011).
- [16] P. J. Digby, *J. Appl. Mech.* **48**, 803 (1981).
- [17] J. D. Goddard, *Proc. R. Soc. Lond. A* **430**, 105 (1990).
- [18] G. McDowell and A. Humphreys, *Granular Matter* **4**, 1 (2002).
- [19] C. Baxter and J. Mitchell, *J. Geotech. Geoenviron. Eng.* **130**, 1051 (2004).
- [20] J. H. Schmertmann, *J. Geotech. Eng.* **117**, 1288 (1991).
- [21] N. Yagi and Y. Iishi, *Bull. Disaster Prev. Res. Inst., Kyoto Univ.* **18**, 15 (1969).
- [22] S. Maqbool, T. Sato, and J. Koseki, in *Soil Stress-Strain Behavior: Measurement, Modeling and Analysis; A Collection of Papers of the Geotechnical Symposium in Rome, March 16-17, 2006*, edited by H. I. Ling, L. Callisto, D. Leshchinsky, and J. Koseki, Solid Mechanics and Its Applications Vol. 146 (Springer, Netherlands, 2007), pp. 595–604.
- [23] J. S. Popovics, ACI-CRC Final Report, 2008.
- [24] E. Fjaer, *Geophysics* **74**, WA103 (2009).
- [25] T. Wichtmann and T. Triantafyllidis, special issue *S1 Geotechnical Engineering of Bautechnik* **86**, 28 (2009).
- [26] B. O. Hardin, *Proceedings of Specialty Conference on Earthquake Engineering and Soil Dynamics* (American Society of Civil Engineering, New York, 1978), pp. 3–90.
- [27] F. Tatsuoka, R. Jardine, D. Lo Presti, H. Di Benedetto, and T. Kodaka, *Proceedings of the XIVth International Conference on Soil Mechanics and Foundation Engineering, Hamburg, 1997* (Balkema, Rotterdam, 1997).
- [28] C. Sauzeat, Doctoral thesis, INSA Lyon, 2003.
- [29] A. Duttine, Doctoral thesis, INSA Lyon, 2005.
- [30] R. Kuwano and R. Jardine, *Can. Geotech. J.* **39**, 1061 (2002).
- [31] P. Lade and C.-T. Liu, *J. Eng. Mech.* **124**, 912 (1998).
- [32] Y. Bréchet and Y. Estrin, *Scr. Metall. Mater.* **30**, 1449 (1994).
- [33] P. Berthoud, C. G'Sell, and J.-M. Hiver, *J. Phys. D* **32**, 2923 (1999).
- [34] L. Bureau, T. Baumberger, and C. Caroli, *Eur. Phys. J. E.* **8**, 331 (2002).
- [35] T. Putelat, J. Dawes, and J. Willis, *J. Mech. Phys. Solids* **59**, 1062 (2011).
- [36] K. L. Johnson, *Contact Mechanics* (Cambridge University Press, Cambridge, 1985).
- [37] G. McDowell and J. Khan, *Granular Matter* **5**, 115 (2003).
- [38] J. Brujić, P. Wang, C. Song, D. L. Johnson, O. Sindt, and H. A. Makse, *Phys. Rev. Lett.* **95**, 128001 (2005).
- [39] H. A. Makse, N. Gland, D. L. Johnson, and L. Schwartz, *Phys. Rev. E* **70**, 061302 (2004).